NEW COMPACT SETUP FOR THERMAL DIFFUSIVITY MEASUREMENT BY PHOTOTHERMAL DEFLECTION TECHNIQUE

M. Bertolotti[1,3], G.L. Liakhou[2], R. Li Voti[1], S. Paoloni[1],
C. Sibilia[1] and V.P. Yakovlev[2]

1 Dipartimento di Energetica, Università di Roma "*La Sapienza*",
Via Scarpa 16, 00161, Roma, Italy,
GNEQP of CNR and INFM, Italy
Tel:+39 6 49916541, Fax:+39 6 44240183
Email: bertolotti@axrma.uniroma1.it

2 Technical University of Moldova,
Stefan Cel Mare 168, 277012 Kishinau, Moldova

3 To whom correspondence should be addressed

ABSTRACT

Photothermal deflection technique applied in harmonic regime allows a careful measurement of the thermal diffusivity of materials. The standard setup is here reviewed together with its main limitations and sources of error. The introduction of a new compact setup, here described, solves some traditional disadvantages making possible the thermal diffusivity measurement also for wide samples.

KEY WORDS: photothermal deflection technique; semiconductor; thermal diffusivity; thermal diffusion length.

1. INTRODUCTION

Thermal diffusivity is the physical quantity which characterizes the heat diffusion process due to the conduction. A direct measurement of this quantity can be performed by using *unsteady methods* only [1]. All methods allow one to estimate the diffusivity by studying the temperature induced when the sample is heated in an unsteady way (*pulsed methods*, *periodical methods* and *monotonic methods*). The use of a laser as heater improved these methods, giving rise to a contactless point-like heating (*photothermal technique* [2]). Concerning the evaluation of the induced temperature, the main improvement has been the use of remote detection systems instead of the standard thermal sensors (*i.e. thermocouple*). In fact they can detect very precisely small temperature rises ($<10^{-6}$ K) through some physical effects connected to the heating, such as the infrared radiation emitted by the sample (*radiometry* [3]), the induced acoustic waves (*photoacoustic* [4]) or the mirage effect (*photothermal deflection* [5]). The last effect refers to a laser beam travelling close to the heated sample, in the air layer where thermal gradients take place. The beam bends towards the colder air layer, giving rise to well known optical illusions (*mirage*). Mirage effect is the working principle for all photothermal deflection devices. Such devices are made of two laser beams (see fig.1). The first laser beam (*pump beam*), used as heat source, is focused onto the sample surface (S) by an optical system of lenses (L_1) and mirrors (M). Eventually the beam is absorbed and the generated heat diffuses into the sample and in the surrounding air. As a consequence of the temperature rise, air refractive index changes are produced. The second laser beam (*probe beam*) is used to detect the temperature field. It is expanded (BE) and focused by a lens (L_2), travels in air skimming the sample surface at a given distance z from it *(vertical offset*) and at a distance y (*horizontal offset*) from the centre of the pump beam. The local changes of the air refractive index n due to the induced heating, cause a weak deflection of the probe beam generally less than one millionth of radian.

The angular deviation is in a plane orthogonal to the probe beam propagation direction, and can be decomposed into two components one *lateral* (Φ_t) and the other one *vertical*

(Φ_n) (see figure 1a). Generally Φ_n is not used for thermal diffusivity measurement because it is too sensitive to the air thermal parameters so that Φ_t is the only used in such application, for which one can write the formula

$$\Phi_t = \frac{1}{n}\left(\frac{dn}{dT}\right)\int_{path}\frac{\partial T}{\partial y}dx \qquad (1)$$

where *dn/dT* is the optothermal coefficient (in air is about -10^{-6} K^{-1}), *n* the air refractive index, *T* the temperature rise. Therefore the deflected probe beam passes through an interferential filter (*IF*), which stops the undesired wavelengths, and impinges on a position sensor (*PS*) which reveals the final beam deflection. Finally *PS* is connected to a lock-in amplifier (*LA*) and a PC-IBM. In figure 1b the electronic system is in the box.

This is the basic setup to detect the mirage effect. It is worth to note that to perform thermal diffusivity measurement [6,7] a heating timer system (*MC, MCD*) and translation stages to move the beams (*SMD*) are also requested. In particular to perform the periodical heating, the pump beam passes through a mechanical modulator (*chopper MC*) or an acousto-optical modulator for frequencies larger than 1 KHz. Moreover to measure the thermal diffusivity it is necessary to follow how the temperature or Φ_t decrease with the distance *y*. The standard procedure is therefore to perform a large number (**Error! Bookmark not defined.**100) of deflection measurements by moving the relative position between the two beams with micrometric movements of the mirror (*SMD*).

2. THERMAL DIFFUSIVITY MEASUREMENTS

The idea for measuring the thermal diffusivity of homogeneous samples with periodical methods immediately comes out looking at the formula of the temperature rise in the ideal case of point-like heating. In other words when a pump beam intensity modulated at the frequency $\omega/2\pi$ is perfectly focused in one point of the sample surface the temperature oscillating at the same frequency is

$$T(r,t) = \frac{P}{2\pi k r} e^{-r/l} \cos(\omega t - r/l) \tag{2}$$

where *P* is the absorbed power, *k* the sample thermal conductivity, *r* the distance from the heating point and l the sample thermal diffusion length defined by $l = \sqrt{2D/\omega}$, where *D* is the sample thermal diffusivity. Eq.(2) clarifies that the temperature rise is a wave damped with the distance from the source. The thermal diffusion length l represents the extinction length of such undulatory process. Looking at the phase of the temperature rise, we note that it is proportional to the distance from the source *r*, according to the simple fact that the phase in one point is connected to the delay needed by the heat diffusion to reach it. This consideration suggest how to perform an accurate measurement of l. Experimentally the phase is measured for different distances *r*. Looking at the plot, in the ideal case, with the least square method, one can work out the interpolator straight line. From its slope that is $m = -1/l$, the thermal diffusion length and hence the thermal diffusivity are calculated. In an analogous way it has been shown that this procedure is still useful also for the phase of Φ_t [6] (*phase method*). Combining Eqs.(1)-(2) one obtains

$$\Phi_t(y,t) = \left|\Phi_t(y,\omega)\right| \cos(\omega t - r/l + \varphi) \tag{3}$$

where *y* is the horizontal offset between the two beams and φ is an unessential phase factor. As an example in fig.2 the phase of the lateral deflection signal for an Indium Phosphide thick sample heated at 900 Hz is shown. The phase tends to the linear behaviour shown in Eq.(3) after the first hundreds of micron. The initial nonlinear behaviour depends on the non-ideality of the experiment which is due to three different reasons. The pump beam is focused not exactly in a point but in a region of finite dimension *a* (typically tens of micron) and it is absorbed not totally at the surface but penetrates also in depth, depending on the absorption coefficient α. Moreover the probe beam cannot touch the sample but just skims over it at a fixed height *z* typically not less than 100 μm. The theoretical study on the lateral component clarifies that all these

reasons distort the phase at small distances from the source while Eq.(3) is still valid for larger ones. In this case the *phase method* can be anyway applied but only in the linear region, giving an estimate of the sample thermal diffusion length which is called *characteristic length* l_c to be distinguished from the real value l. The causes for which l_c differs from l are due both to causal and well identified systematic errors. These last ones depend on the parameters a, α, z and can be corrected by using an additional procedure later described. Coming back to the example shown in fig.2, it is important to have an idea on the casual errors. In figure 3 the variance on the phase data obtained by repeating 15 times the same measurement, is plotted as a function of *y*. Note that the uncertainty is generally less than one degree and increases weakly with the distance. In $y=0$ the variance has its maximum value due to the fact that the amplitude of the lateral deflection should go to zero so that the phase fluctuates. Anyway the casual errors cannot change the asymptotic linear behaviour of Fig.2 so that it is possible, by using the least square method, to find out the characteristic length that is l_c= 126.4 ± 0.4 μm. Note that the casual errors cause an uncertainty smaller than 0.4 % which is almost negligible for a 30 points scan in *y* already. From l_c , being $l \cong l_c$, one could obtain directly the thermal diffusivity by using the formula $D = \pi \quad f \quad l^2$ which gives a value D=0.450 cm^2/s. Indeed this procedure is not correct because it does not take into account the systematic errors for l which double the error of *D*. These systematic errors are the main source of uncertainty and, for samples with thermal diffusivity smaller than the air one (D<0.2 cm^2/s), can lead to a wrong evaluation of *D*. It is worth to summarise here the known systematic errors discussing their influence on the measurement.

1) Systematic error due to the absorption α.

This error occurs when the pump beam is gradually absorbed in depth. The phase plot in *y* differs, at small *y*, from the ideal straight line. Therefore it is possible again to apply the least square method starting from a distance y_o from the source. The value obtained for l_c differs from the real one l depending on the value of y_o. Of course the farer we move from the heating region, the lower is the difference between l_c and l and hence

this systematic error. A useful point of view is to fix the value of the tolerable error and to plot the minimum distance y_O at which the systematic error is under the fixed threshold. In figure 4 the minimum distance normalized to the thermal diffusion length y_O/l is plotted as a function of the absorption normalized to the thermal diffusion length αl for two values of the relative tolerable error (3% and 10%). From the graph it is clear that the systematic error changes with absorption; in particular for a transparent sample (αl<0.1) it is negligible, while for opaque samples it can be anyway reduced to less than 3% choosing the starting distance larger than two times l. In theory taking into account larger distances one could have a further reduction of this error but in practice this is prevented by the casual error which increases and becomes dominant at large distances.

2) Systematic error due to the pump spot size *a*.

A phase distortion for small *y* again occurs when the heating source has a finite size *a*. Anyway the *phase method* can be applied, as in the previous case, starting from an initial distance y_O. The systematic error depends again on the value of y_O but the theory guarantees that it can be kept to less than 3% just choosing y_O larger than two times *a*.

3) Systematic error due to the vertical offset *z*.

This is the most serious systematic error. It is worth to note that if the probe beam travels in air at a distance *z* from the surface too high with respect to the thermal diffusion length l, any photothermal signal can "*loose*" the information on the sample diffusivity. In practice, by increasing *z* up to some thermal diffusion length, the signal still *"feels"* the sample; the phase plot has the usual initial distortion and, for large *y*, behaves, as usual, like a straight line. Looking at its slope one finds a characteristic length l_c which can substantially differ from l for low diffusivity samples. This systematic error cannot be in any case reduced by moving the starting distance y_O. The numerical simulations have shown that this error is negligible only for high diffusivity samples (*D>0.2*), while for low diffusivity samples (*D<0.2*) l_c increases with *z* according to the formula [6]

$$l_c = l + \frac{z}{4}\sqrt{\frac{D_{air}}{D}} \quad \Rightarrow \quad l_c = \sqrt{D/\pi}\sqrt{1/f} + \frac{z}{4}\sqrt{\frac{D_{air}}{D}} \tag{4}$$

valid for z is smaller than some and $D<D_{air}$. In other words l_c is given by the sum of two terms: one given by l which depends only on the frequency as $1/\sqrt{f}$ and the other undesired term which is independent on the frequency and increases with z and the thermal diffusivity mismatch D_{air}/D. The method to correct this serious error is based on the frequency discrimination. By applying the phase method for different frequencies and plotting the characteristic length as a function of $1/\sqrt{f}$, a straight line is obtained whose slope is $\sqrt{D/\pi}$, a quantity directly connected to the sample diffusivity. Therefore to estimate the diffusivity one has to apply the least square method to the l_c data as a function of $1/\sqrt{f}$, calculate the slope $\Delta l_c/\Delta(1/\sqrt{f})$ and determine D through the formula

$$D = \pi\left(\frac{\Delta l_c}{\Delta\sqrt{1/f}}\right)^2 . \tag{5}$$

Indeed this method, thought for low diffusivity sample, is used for any sample. In fact the frequency discrimination allows to correct also other minor systematic errors due to all geometrical misalignments which could add to l_c some frequency independent terms.

As an example in figures 5 and 6 this procedure is shown for the same Indium Phosphide sample of fig.3. The phase vs the offset y is plotted for different frequencies in fig.5. Note that a linear region always occurs starting from *y=0.1 mm*. From the five slopes, the characteristic lengths are worked out and plotted in figure 6 as a function of $1/\sqrt{f}$. From these data one can trace a second straight line from which, according to Eq.5, the Indium Phosphide diffusivity of D = 0.428 ± 0.007 cm^2/s is found. It is worth to note that this method can be used only when the height z is smaller than some thermal diffusion length and Eq.(4) is still valid. To overcome this limitation the recent efforts have been directed towards the realisation of compact devices which minimise the undesired quantity z and guarantee the best estimate for D in any experimental condition.

3. NEW COMPACT SETUP

The crucial point of the traditional photothermal deflection systems is that the probe beam has to travel at a distance from the surface which has to increase with the sample size giving rise to systematic errors in the diffusivity measurement. To overcome this limitation a new setup has been planned and realised in which the height *z* from the surface is fixed independently on the sample size (see figure 7). The new compact device, realised in our laboratories [7], is made of a sample holder (2 in fig.7) on which two prisms are mounted at 6 mm from each other (1 in fig.7) which can drive the probe beam path at the fixed height of 50 ± 3 μm. If a smaller height is needed one has to reduce the probe beam waste and hence the probe beam path over the sample, simply decreasing the distance between the two prisms. Of course this is possible till the distance between the prisms does not interfere with the experiment. The technical novelty is in the used prisms, obtained by cutting the semiconductor wafer in the crystallographic direction <1 1 1>. This cheap procedure guarantees the sharpened prism edges needed to keep as close as possible to the surface. Finally to measure the thermal diffusivity the same method and criteria described in section 2 can be applied. The new device has been tested on different monocrystal semiconductors with known thermal diffusivity (see Tab.1). The dimensions of these samples are so wide that no way exists to apply standard photothermal deflection systems. By comparing the measured diffusivities with the ones given in literature we found a good agreement [1].

4. CONCLUSIONS

The *phase method* to measure the thermal diffusivity of materials by the photothermal deflection technique has been reviewed. The main limitation of the standard device due to the probe beam height has been put into evidence so to justify the plan and the realisation of a new compact setup which has been tested on samples whose dimensions prevent from applying the standard techniques.

REFERENCES

1 Y.S. Touloukian , R.W. Powell, C.Y. Yo and M.C. Nicolaou, in *Thermophysical Properties of Matter*, Vol.10 *Thermal Diffusivity*, Plenum Press (1973).

2 A.C. Tam, *Rev Mod. Phys.* **58**: 381 (1986).

3 P.E.Nordal, S.O.Kanstad, *Physica Scripta* **20**: 659 (1979).

4 A.Rosencwaig, A.Gersho, *J.Appl.Phys.* **47**: 64 (1976).

5 A.C.Boccara, D.Fournier, W.B.Jackson, N.M.Amer, *Optics Letters* **l5**:377(1980)

6 M.Bertolotti, G.L.Liakhou, R.Li Voti, C.Sibilia, *Rev Sci.Instrum*, **64**:1576(1993)

7 M. Bertolotti, V. Dorogan, G.L. Liakhou, R. Li Voti, S.Paoloni and C.Sibilia, *Rev Sci.Instrum.* **68:** (1997).

Table I: Experimental Results on Thermal diffusivity Measurements

Sample	D measured (cm^2/s)	D litterature (cm^2/s)
InSb	0.19	0.19
InAs	0.21	0.19
InP	0.44	0.46
GaAs	0.25	0.25
GaP	0.45	0.45
Ge	0.38	0.37
Si	0.80	0.88

CAPTION FOR FIGURES

Figure 1: Schematic representation of the standard photothermal deflection setup:

(a) laser beam geometry;

(b) basic experimental setup.

Figure 2: Phase (degree) of the lateral deflection signal as a function of *y* (mm) for an homogeneous Indium Phosphide thick sample. The frequency is 900 Hz and the sample thermal diffusion length is 126 μm.

Figure 3: Casual error: variance of the data in fig.2.

Figure 4: Systematic error due to α. Distance normalised to the thermal diffusion length which guarantees a relative error of 3% and 10% respectively. The graphs are plotted as a function of the parameter αl.

Figure 5: Phase (degree) of the lateral deflection signal as a function of *y* (mm) for the same sample in fig.2. The five graphs refer to different frequencies (• 225 Hz , + 400 Hz, ◊ 625 Hz, Δ 900 Hz, x 1600 Hz)

Figure 6: The characteristic lengths (micron) obtained from the data in fig.5 are plotted as a function of the inverse square root of frequency ($Hz^{-1/2}$). The continuos line is the interpolator line given by the least square method.

Figure 7: Scheme of the new compact setup for the thermal diffusivity measurements. The prisms have been prepared from GaP <1 1 1> wafers.

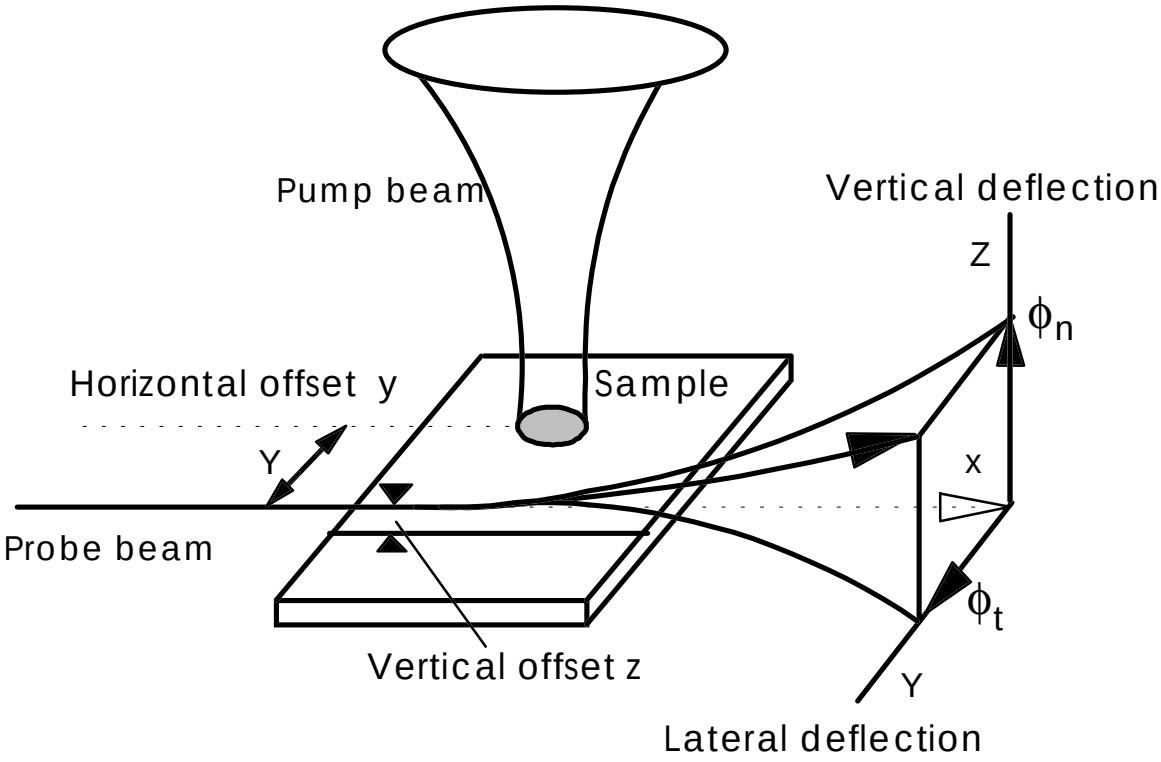

Figure 1a

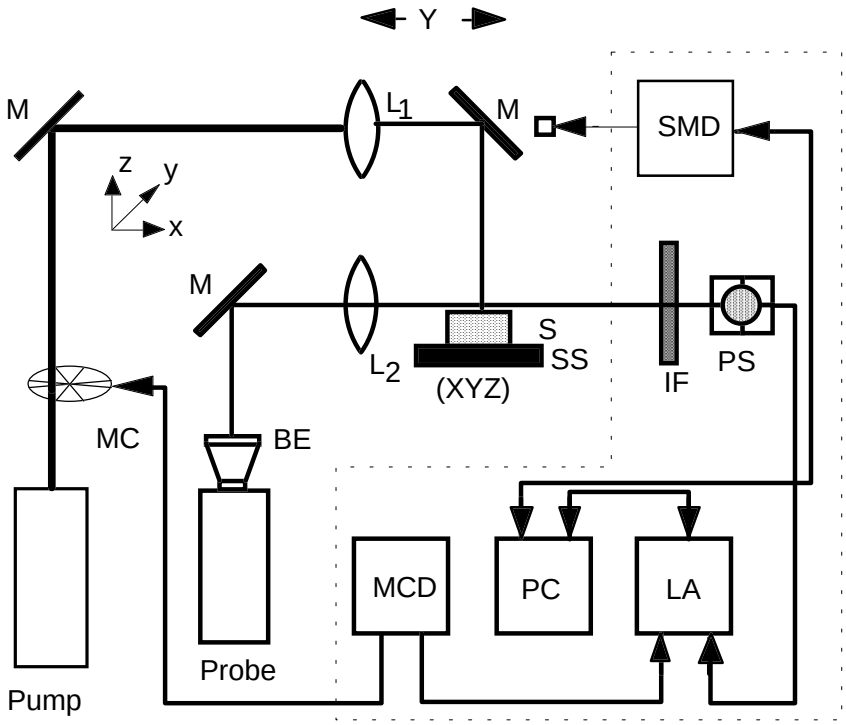

Figure 1b

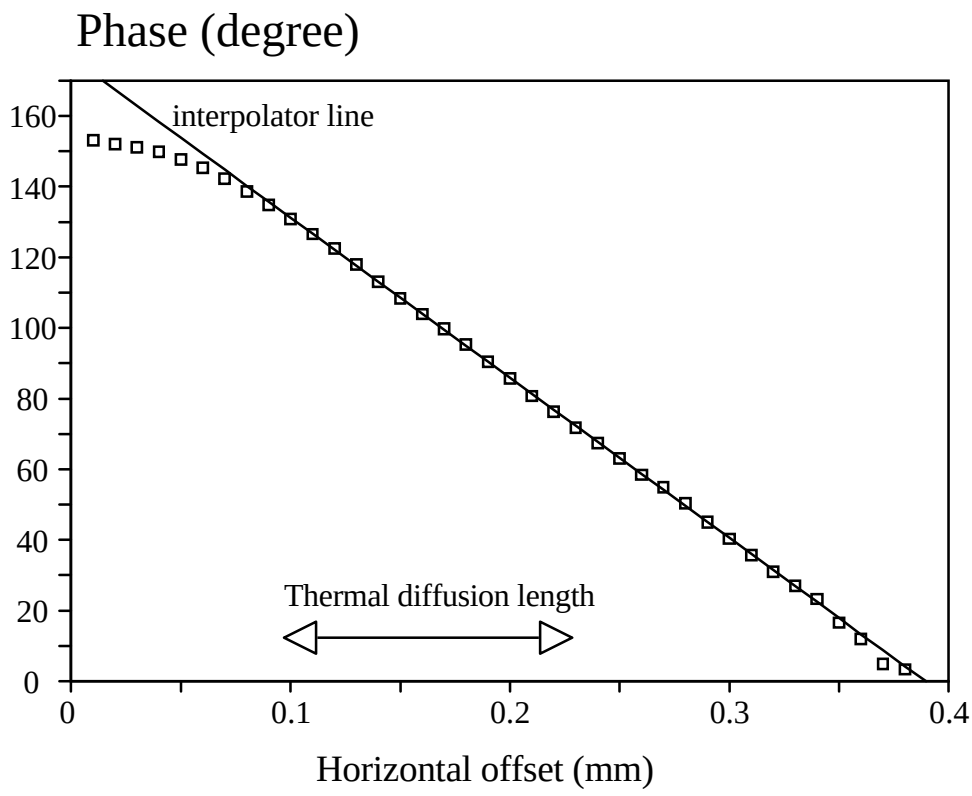

Figure 2

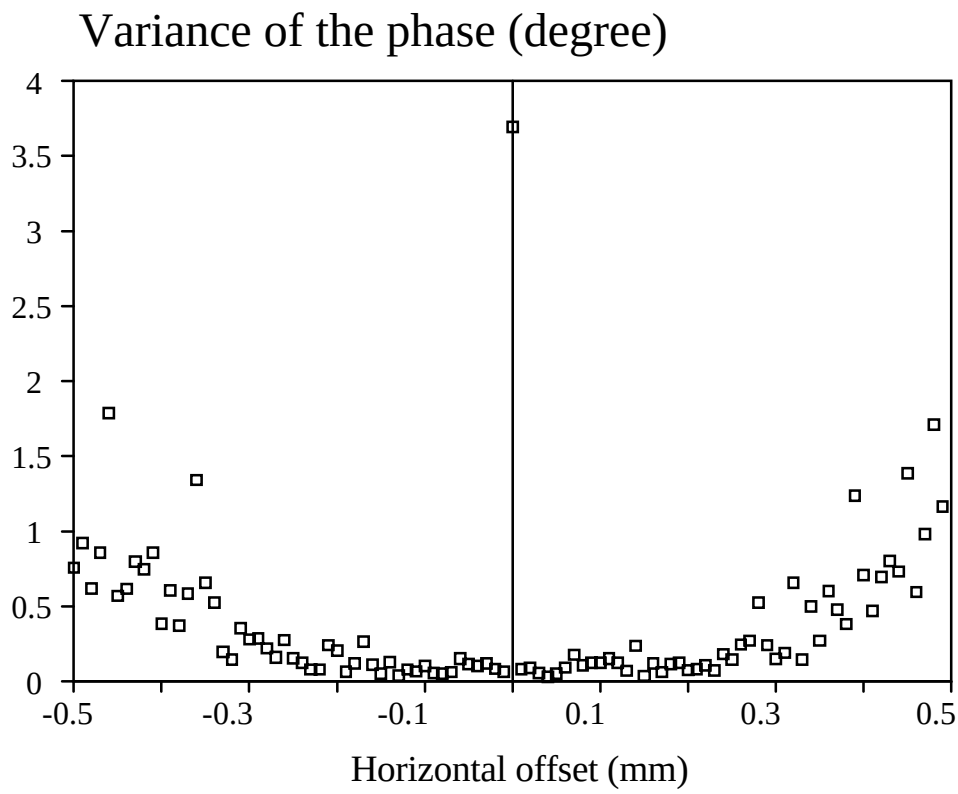

Figure 3

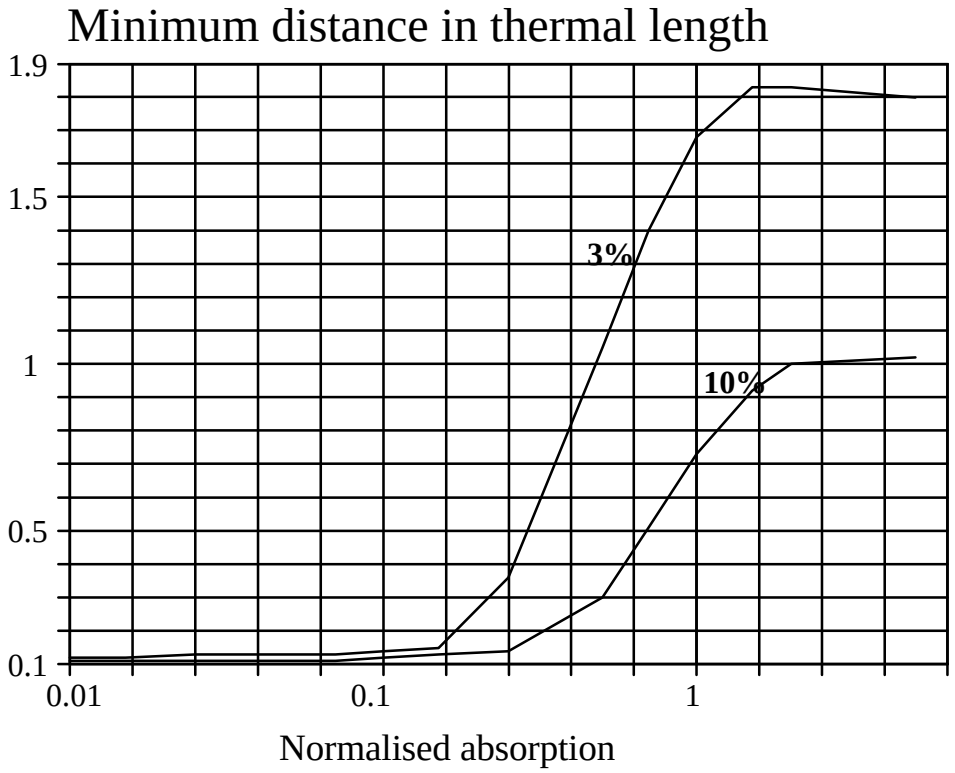

Figure 4

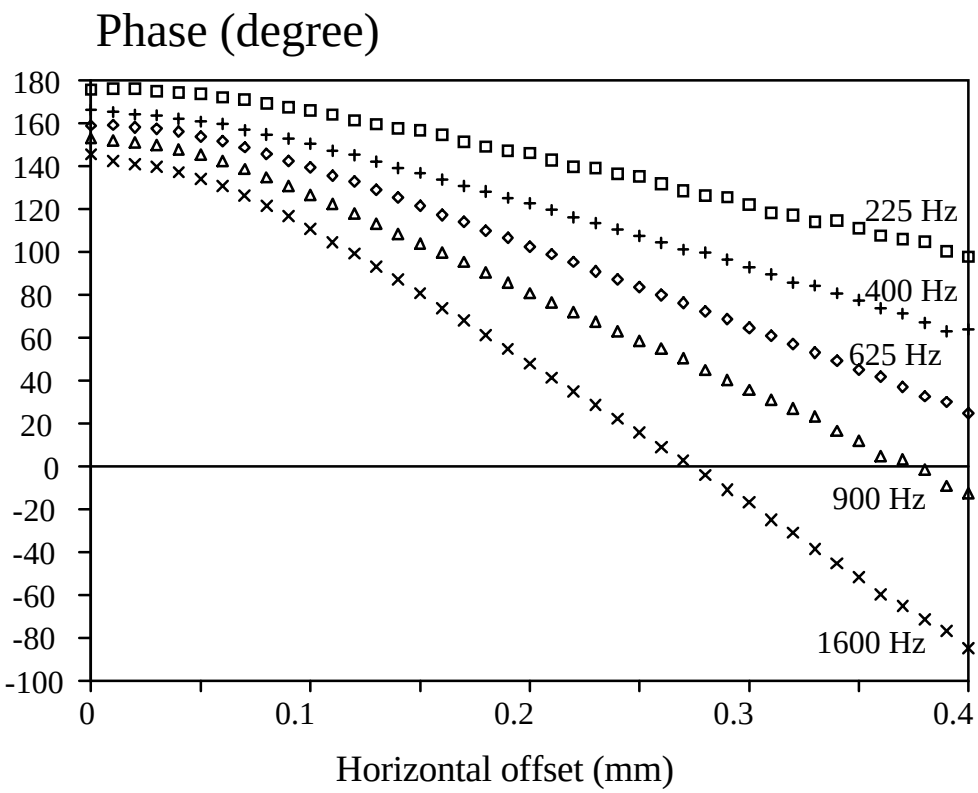

Figure 5

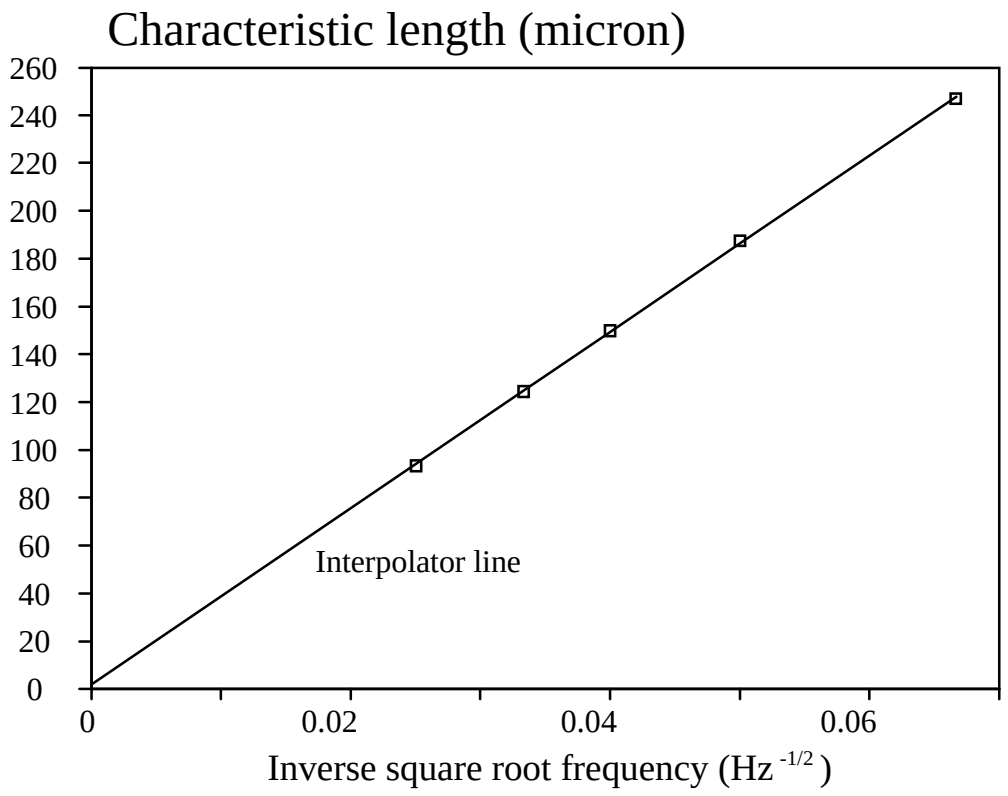

Figure 6

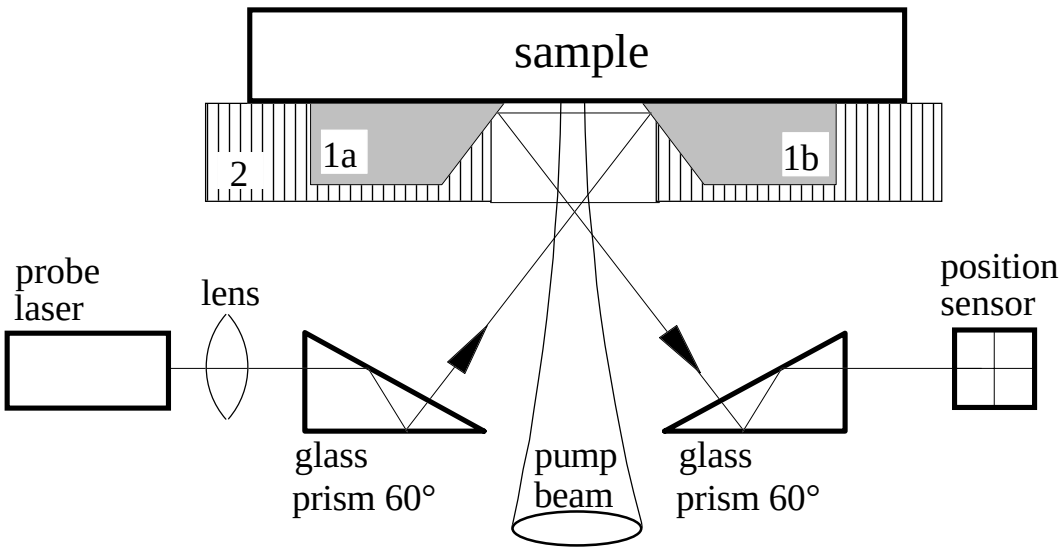

Figure 7